ANSYS investigation of solar photovoltaic temperature distribution for improved efficiency

Paul Rousseau, Hassan Nouri
School of Engineering, Power System and Energy Research Laboratory, University of the West of England, Frenchay Campus, Bristol, United Kingdom

Article Info	ABSTRACT
	A computational analysis of the influence of varying solar module material properties on operating temperature is presented and related to electrical conversion efficiency through the devised method. By varying the properties of density, specific heat capacity, and isotropic thermal conductivity for each material that comprises a solar module, density, and specific heat capacity were found to have the greatest influence on decreasing the operating temperature when increased by a factor of 50% for the glass layer, resulting in a decrease in temperature of 5.33 °C. Utilizing the devised method, which is based on the work of Palumbo, this temperature decrease was correlated to an electrical efficiency increase of 3.08%.

Corresponding Author:

Paul Rousseau
School of Engineering, Power System and Energy Research Laboratory, University of the West of England, Frenchay Campus
Coldharbour Ln, Stoke Gifford, Bristol BS16 1QY, United Kingdom
Email: prousseau310@gmail.com

1. INTRODUCTION

Due to rapid industrialization and an ever-increasing human population, with an estimated growth in world population from 7 billion in 2013 to 9.4 billion by 2050, it is estimated that there will be a subsequent increase in energy consumption from 546 EJ in 2010 to 879 EJ by 2050 [1]. As of 2015, over 85% of the global energy mix came from the burning of harmful fossil fuels [2]. Utilizing renewable energies, for example, solar photovoltaic (PV), as a means to reduce our fossil fuel consumption, is paramount for the longevity of humanity and the planet due to the inherent problems associated with fossil fuels.

Solar PV converts incoming solar irradiation into electricity through a process known as the photovoltaic effect. The biggest factor that limits the viability of solar PV however is the negative effect that operating cell temperature has on the already low PV energy conversion rate. An increase in cell temperature decreases open circuit voltage, resulting in a drop in electrical efficiency. This relationship is based on the general diode equation that expresses the behavior of a simple PV system [3]. In addition to efficiency losses, these increases in temperature cause thermal stresses to occur in the PV module which lead to permanent structural damage over time, hence reducing the PV module lifetime [4].

Significant effort has been made to increase efficiency via operating temperature reduction through various means, such as forced fluid cooling [5]–[7] radiative cooling techniques via transparent coatings [8], [9] incorporating phase-change materials on the back of the solar module [10]–[12] submerging PV modules in bodies of water [13]. Despite these previous efforts reported so far, there has been no investigation into the effect the material properties of each constituent solar module material have on its operating surface

temperature. This study aims to computationally investigate the effect of material properties of each constituent solar module material on its operating surface temperature, output power, and efficiency. Section 2 of the paper discusses the Palumbo modeling approaches in ansys and its adaptation for this study and section 3 discusses the thermal simulation method for various material densities, thermal conductivities, and heat capacities. Also discussed is the efficiency derivation of the module. Section 4 demonstrates the results of the simulation model. Finally, section 5 concludes this investigation.

2. MODELLING VALIDATION AND ADAPTATION

In this section, Palumbo's work [14] will be reproduced to ensure the validity of our ANSYS model. This will also enable its adaptation for the study of surface temperature, I-V and P-V characteristics, and increased efficiency of the solar panel. This in turn will require knowledge of material properties, boundary conditions, selection of appropriate mesh size, shape, nodes, solver, and simulation time step.

2.1. Production of Palumbo's model

The Chosen model to reproduce from Palumbo's work was the "2D, bare panel, natural convection" model. The model was recreated using the steady-state thermal analysis system contained in the ANSYS software. The solar module layers and their respective thicknesses were created with the values from Table 1 which, according to Palumbo, are typical for solar panels. Further research was done by others confirming the validity of these values [15], [16]. The arc layer was omitted under the assumption its effect on the model would be negligible due to its extremely miniscule thermal resistance. The model was then meshed with a total number of grid elements and nodes of 2,528 and 14,408 respectively and is shown in Figure 1.

Table 1. Palumbo's solar module material properties and layer thicknesses

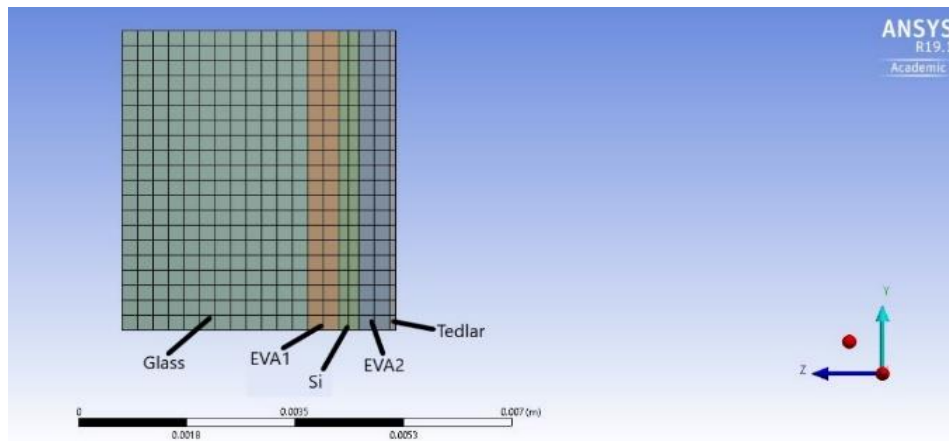| Material	Conductivity (W/m.K)	Thickness (m)
Glass	0.98	0.003
Eva 1	0.23	0.0005
Arc	1.38	0.08×10^{-6}
Si	148	0.000325
Eva 2	0.23	0.0005
Tedlar	0.36	0.0001

Figure 1. Palumbo's model reproduction mesh

The boundary conditions used in Palumbo's model are as i) an Irradiance of 1000 W/m^2 was applied to the top face of the glass layer using the heat flux boundary condition, ii) a convection load was applied to the top face of the glass layer and bottom face of the tedlar layer with the ambient temperature and film coefficient being set to 22 °C and 3.50 W/m^{2}K respectively. The value for the film coefficient was obtained through experimental calculations done by Palumbo, iii) a perfect insulation boundary condition was applied to the side faces of the model as it is assumed that heat transfer will only take place through the thickness of the model. i.e. 2D.

The simulation was then run and the results were compared to those obtained by Palumbo. The comparative results of the front glass layer and back tedlar layer are shown in Table 2. The replicated results and Palumbo's results were found to differ by 1% and 2.5% for the top layer and bottom layer respectively. This difference is believed to be due to changes in the ansys software since Palumbo carried out his study and as such the model was deemed to be valid.

2.2. Adapted model

Due to steady-state thermal analysis only allowing the material property of isotropic thermal conductivity to be used, it was deemed necessary to use the transient thermal analysis instead to accommodate the material properties of density and specific heat capacity. The values are shown in Table 3, with the only changes being the addition of the density and specific heat capacity material properties. The timestep of this model was set to 180 seconds to produce a noticeable change in temperature. Apart from this the other boundary conditions used in Palumbo's report remained the same. The electrical characteristics of the solar module used in Palumbo's experimental work are shown in Table 4. These characteristics are used throughout section 3 for the derivation methods.

Table 2. Comparative thermal results

Model	Temperature (front) °C	Temperature (back) °C
Palumbo (analytical)	169.53	165.66
Palumbo (ansys)	168.35	166.80
Authors template	166.75	162.96

Table 3. Adapted solar module material properties and layer thicknesses

Material	Density (Kg/m^3)	Thermal conductivity (W/mK)	Specific heat capacity (J/Kg°C)	Thickness (m)
Glass	3,000	0.98	500	0.003
Eva1	960	0.23	2090	0.005
Silicon	2,330	148	677	0.000325
Eva2	960	0.23	2090	0.005
Tedlar	1200	0.36	1250	0.0001

Table 4. Palumbo's solar module's electrical characteristics

P_{mpp} (W)	V_{mpp} (V)	I_{mpp} (A)	V_{OC} (V)	I_{SC} (A)	η_{max} (%)
10	17.4	0.57	21.6	0.64	8.8

3. SIMULATION AND DERIVATION METHOD

This section explains the method used to construct the ansys models and correlate temperature change to PV conversion efficiency. Furthermore, the correlation of PV conversion efficiency change to the I-V and P-V curves will be described. Attempts are also made to derive an expression for the efficiency from the results obtained in the simulation.

3.1. Thermal simulation method

Simulations are performed with the material properties of density, thermal conductivity, and heat capacity being varied, independently of each other over a range of -15% to +50% of their initial values in increments of 5%. This is carried out for each material while keeping the properties of the other materials fixed at their original values. The maximum and minimum temperature for each of these simulations is recorded.

3.2. Efficiency derivation

Palumbo's experiments are carried out for irradiance values of 1,000 W/m^2, 1,250 W/m^2, and 1,500 W/m^2. Then from the experimental results, Palumbo correlated values of output power are plotted against changes in surface temperature as shown in Figure 2. Also, Figure 2 presents the equations of power-temperature lines.

It is clear to see that the equation of lines provided by Palumbo in Figure 2 can be rewritten as (1).

$$P_{Out} = mT_S + C \tag{1}$$

Where P_{Out}, T_S, and C are output power, surface temperature, and y-intercept respectively.

The line equation for the irradiance value of 1000W/m^2 from Figure 2 is used and adapted as (2).

$$P_{Out} = -0.018T_S + 3.8687 \qquad (2)$$

The electrical characteristics of the solar module used in Palumbo's experimental analysis are defined in Table 4 as Pmax = 10 W and $\eta_{PV,max}$ = 8.8%. Using (3), the input power for an irradiance of 1000 W/m^2 was found to be 113.6 W.

$$P_{In} = \frac{P_{max}}{\eta_{PV}} \qquad (3)$$

The temperature changes as a result of varying the material properties for the solar module materials of glass, ethylene vinyl acetate (EVA), and silicon, and are now able to be related to an efficiency increase using (4).

$$\Delta\eta = \frac{\Delta P_{Out}}{P_{in}} = \frac{P_{Out,altered} - P_{Out,baseline}}{113.6} \qquad (4)$$

Where P$_{out,altered}$ and P$_{out,baseline}$, are the output power of a model where the material property is altered and the output power of the baseline model where no material properties are altered respectively.
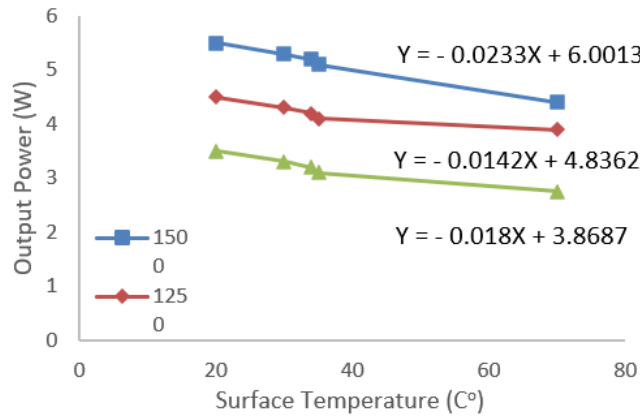

Figure 2. Correlation of output power and surface temperature for bare panel [14]

3.3. I-V and P-V curve characteristics

Using the output power values calculated in section 3.2, the output voltages are found using (5), thus relating them to temperature change as a result of varying material properties. The output current is fixed at I$_{out}$ = 0.57 A. It has been well documented that changes in operating temperature have very little effect on the output current of solar cells in comparison to their output voltage, therefore any errors that may arise from the previous assumption are deemed small enough to be negligible [17].

$$V_{Out} = \frac{P_{out}}{0.57} \qquad (5)$$

According to researchers [18]–[20] three key physical quantities shown in Table 5 must be defined to determine the I-V curve characteristics of a PV cell, namely, open-circuit voltage (V$_{OC}$), short-circuit current (I$_{SC}$) and the output current and output voltage that permits the maximum power (P$_{mpp}$) to be obtained. As stated earlier, I$_{SC}$ will vary very little with temperature change so is assumed to be constant at 0.64 A. The percentage difference between V$_{oc}$ and V$_{mpp}$ for the original I-V curve at STC is calculated and found to be approximately 20%. This percentage change is used as a means to approximate the V$_{oc}$ for the I-V curves operating at different temperatures.

Table 5. I-V and P-V characteristic curve coordinate system

Coordinates	I-V Curve Coordinates (x,y)	P-V Curve Coordinates (x,y)
Coordinate 1	$(0, I_{SC})$	$(0,0)$
Coordinate 2	(V_{mpp}, I_{mpp})	$(V_{mpp}, P_{max)}$
Coordinate 3	$(V_{OC}, 0)$	$(0,0)$

4.   RESULTS AND DISCUSSION

4.1. Thermal simulation

Figure 3 illustrates the changes in surface temperature as a result of varying the respective material properties (density, specific heat capacity (SHC), and isotropic thermal conductivity (ITC)) of the glass, EVA, silicon, and tedlar materials using the method explained in section 3.1. From Figure 3(a) (density) and Figure 3(b) SHC, it can be observed that when varying the density and SHC for any four of the materials the relationship with the surface temperature can be seen to be inversely proportional. It should also be noted that the changes in surface temperature as a result of varying density and SHC for all four materials are found to be the same for both material properties with the largest surface temperature decrease of 5.33 °C occurring at +50% for the glass layer. Inspection of Figure 3(c) ITC suggests that when varying ITC, the relationship with surface temperature is only inversely proportional for the glass material while being proportional for the three other materials. It can also be observed that the extent to which varying ITC had on changes in surface temperature is small in comparison to density and SHC with the greatest surface temperature decrease of 0.45 °C occurring at +50% for the glass layer.

(a)   (b)
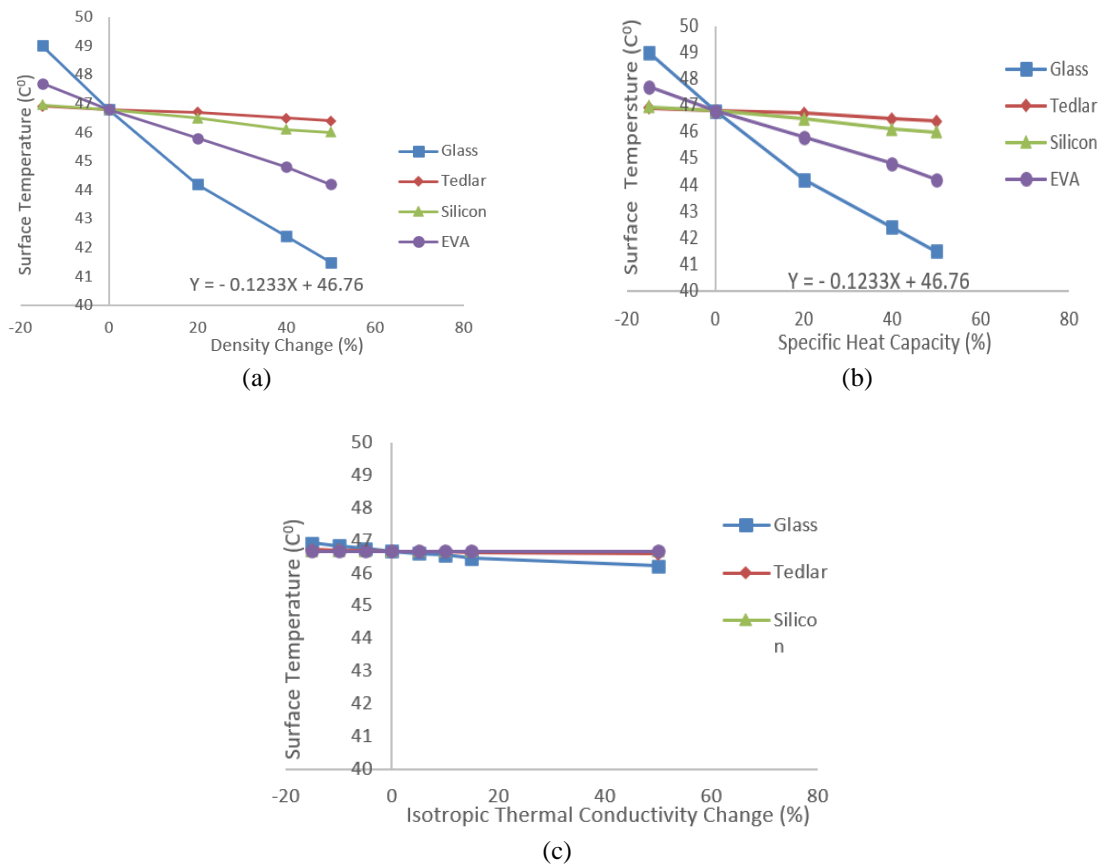

(c)

Figure 3. Surface temperature characteristics against material properties (a) density, (b) specific heat capacity, and (c) isotropic thermal conductivity

4.2. Temperature and efficiency

Using (2) to (4) and the method explained in section 3.2 the changes in surface temperature as a result of varying material properties are related to changes in PV conversion efficiency. The efficiency results for density and SHC are found to be the same due to the thermal results being identical and as such are both

illustrated in Figure 4. A tentative analysis of Figure 4 reveals that efficiency and these material properties share a proportional relationship, with changes in the material properties of the glass material having the largest effect on efficiency change with an efficiency increase of 3.08% occurring at +50%.
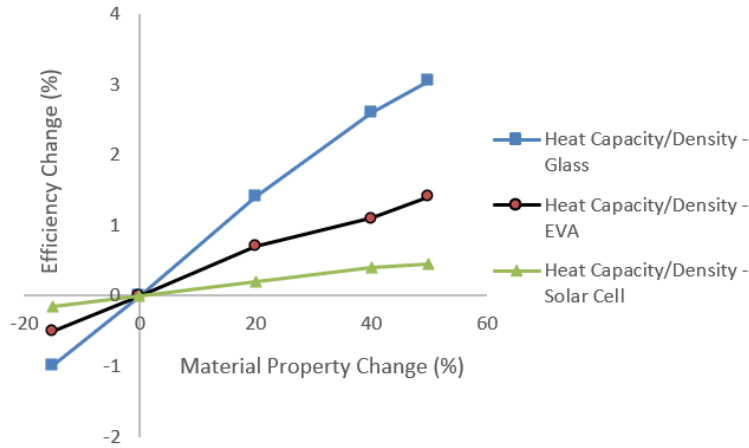
Figure 4. Profile of electrical efficiency against material properties

4.3. Photovoltaic module I-V and P-V characteristics

Using (5) and the method explained in section 3.3, the output voltages of the module are found for each change in material property, which is then used to find the respective maximum power outputs. Figures 5(a) and 5(b) show the resultant I-V and P-V curves of the test scenario respectively where the SHC is increased by 50%. Also shown within these respective figures are the I-V and P-V curves of the reference panel at STC.
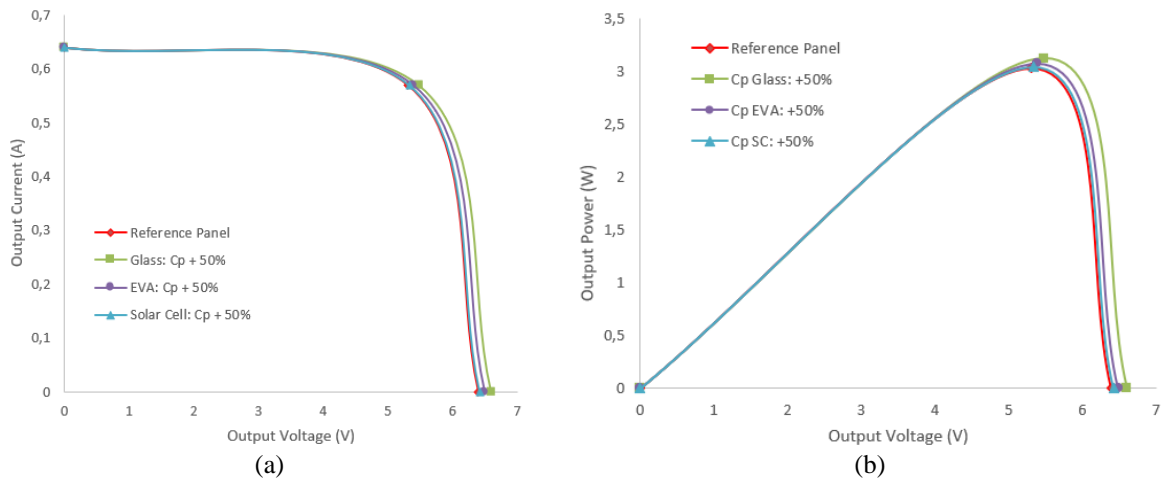
Figure 5. Shows the influence of specific heat capacity of solar panel materials on the output (a) current and output voltage profile and (b) power and output voltage characteristics

5. CONCLUSION

The extent to which varying the material properties of density, thermal conductivity, and specific heat capacity affect the operating temperature of a solar module has been successfully investigated through computational analysis. Increasing the material properties of density, specific heat capacity, and isotropic thermal conductivity by 50% resulted in a surface temperature decrease of 5.33 °C and 0.45 °C respectively, with the thermal reaction being the same for density and specific heat capacity. A method to relate these

temperature changes to PV conversion efficiency is then derived by the authors through the usage of experimental data referenced from the work of Palumbo. Using the aforementioned method and the results from the thermal investigation, an electrical efficiency increase of 3.08% is possible when the density or specific heat capacity of the glass material is increased by 50%. Lastly, a reliable method to determine the shift in the characteristic I-V and P-V curves as a result of varying these material properties is constructed. The results of this investigation provide valuable insight into the extent to which each material and their respective properties influence operating temperature which can be taken into consideration when designing future solar modules to minimize operating temperature via either addition or subtraction of the respective materials. The temperature-efficiency and electrical characteristic methods derived by the authors also provide a valuable method to relate temperature change to efficiency change and approximate key electrical characteristics of solar modules.

ACKNOWLEDGEMENTS

REFERENCES

[1]   World Energy Council, "World Energy Scenarios: Composing energy futures to 2050," *World Energy Council*, pp. 1–288, 2013.
[2]   World Energy Council, "World Energy Resources 2016," *World Energy Council 2016*, pp. 27–29, 2016.
[3]   K. I. Ishibashi, Y. Kimura, and M. Niwano, "An extensively valid and stable method for derivation of all parameters of a solar cell from a single current-voltage characteristic," *Journal of Applied Physics*, vol. 103, no. 9, pp. 1–7, 2008, doi: 10.1063/1.2895396.
[4]   T. T. Chow, "A review on photovoltaic/thermal hybrid solar technology," *Renewable Energy: Four Volume Set*, vol. 4–4, pp. 88–119, 2018, doi: 10.4324/9781315793245-122.
[5]   R. Mazón-Hernández, J. R. García-Cascales, F. Vera-García, A. S. Káiser, and B. Zamora, "Improving the electrical parameters of a photovoltaic panel by means of an induced or forced air stream," *International Journal of Photoenergy*, vol. 2013, pp. 1–10, 2013, doi: 10.1155/2013/830968.
[6]   A. Kroiss, A. Pröbst, S. Hamberger, M. Spinnler, Y. Tripanagnostopoulos, and T. Sattelmayer, "Development of a seawater-proof hybrid photovoltaic/thermal (PV/T) solar collector," *Energy Procedia*, vol. 52, pp. 93–103, 2014, doi: 10.1016/j.egypro.2014.07.058.
[7]   M. Ghadiri, M. Sardarabadi, M. Pasandideh-Fard, and A. J. Moghadam, "Experimental investigation of a PVT system performance using nano ferrofluids," *Energy Conversion and Management*, vol. 103, pp. 468–476, 2015, doi: 10.1016/j.enconman.2015.06.077.
[8]   L. Zhu, A. Raman, K. X. Wang, M. A. Anoma, and S. Fan, "Radiative cooling of solar cells," *Optica*, vol. 1, no. 1, p. 32, 2014, doi: 10.1364/optica.1.000032.
[9]   L. Zhu, A. P. Raman, and S. Fan, "Radiative cooling of solar absorbers using a visibly transparent photonic crystal thermal blackbody," *Proceedings of the National Academy of Sciences of the United States of America*, vol. 112, no. 40, pp. 12282–12287, 2015, doi: 10.1073/pnas.1509453112.
[10]   Z. A. Haidar, J. Orfi, and Z. Kaneesamkandi, "Experimental investigation of evaporative cooling for enhancing photovoltaic panels efficiency," *Results in Physics*, vol. 11, pp. 690–697, 2018, doi: 10.1016/j.rinp.2018.10.016.
[11]   S. D. Sharma, H. Kitano, and K. Sagara, "Phase Change Materials for Low Temperature Solar Thermal Applications," *Res. Rep. Fac. Eng. Mie Univ.*, vol. 29, pp. 31–64, 2004.
[12]   F. Hachem, B. Abdulhay, M. Ramadan, H. El Hage, M. G. El Rab, and M. Khaled, "Improving the performance of photovoltaic cells using pure and combined phase change materials – Experiments and transient energy balance," *Renewable Energy*, vol. 107, pp. 567–575, 2017, doi: 10.1016/j.renene.2017.02.032.
[13]   M. Rosa-Clot, P. Rosa-Clot, G. M. Tina, and P. F. Scandura, "Submerged photovoltaic solar panel: SP2," *Renewable Energy*, vol. 35, no. 8, pp. 1862–1865, 2010, doi: 10.1016/j.renene.2009.10.023.
[14]   A. Palumbo, "Design and Analysis of Cooling Methods for Solar Panels," *Climate Change 2013 - The Physical Science Basis*, no. December 2013, pp. 1–30, 2013.
[15]   C. G. Popovici, S. V. Hudişteanu, T. D. Mateescu, and N. C. Cherecheş, "Efficiency Improvement of Photovoltaic Panels by Using Air Cooled Heat Sinks," *Energy Procedia*, vol. 85, pp. 425–432, 2016, doi: 10.1016/j.egypro.2015.12.223.
[16]   W. Z. Leow, Y. M. Irwan, M. Irwanto, M. Isa, A. R. Amelia, and I. Safwati, "Temperature distribution of three-dimensional photovoltaic panel by using finite element simulation," *International Journal on Advanced Science, Engineering and Information Technology*, vol. 6, no. 5, pp. 607–612, 2016, doi: 10.18517/ijaseit.6.5.926.
[17]   E. Radziemska and E. Klugmann, "Thermally affected parameters of the current-voltage characteristics of silicon photocell," *Energy Conversion and Management*, vol. 43, no. 14, pp. 1889–1900, 2002, doi: 10.1016/S0196-8904(01)00132-7.
[18]   E. Saloux, A. Teyssedou, and M. Sorin, "Explicit model of photovoltaic panels to determine voltages and currents at the maximum power point," *Solar Energy*, vol. 85, no. 5, pp. 713–722, 2011, doi: 10.1016/j.solener.2010.12.022.
[19]   R. Kumar, S. K. Singh, and others, "Solar photovoltaic modeling and simulation: As a renewable energy solution," *Energy Reports*, vol. 4, pp. 701–712, 2018.
[20]   I. A. Moiseev, A. N. Shishkov, I. A. Berseneva, and K. V. Osintzev, "Simulation of the operation of the solar panel of the pilot plant in the Ansys software package," *IOP Conference Series: Earth and Environmental Science*, vol. 990, no. 1, pp. 1–6, 2022, doi: 10.1088/1755-1315/990/1/012059.

BIOGRAPHIES OF AUTHORS

Paul Rousseau 🆔 8ᵍ SC ⟳ has obtained he Bachelor of Engineering in Mechanical Engineering in 2019 from the University of the West of England, United Kingdom. Paul will be completing his postgraduate study in 2023 within the Power Systems and Energy Research Laboratory at the University of the West of England, Bristol. He can be contacted at email: prousseau310@gmail.com.
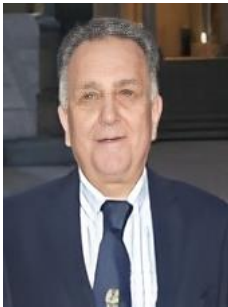
Hassan Nouri 🆔 8ᵍ SC ⟳ Received the B.Sc., M.Sc., and Ph.D. degrees in electrical and electronic engineering from the Universities of Nottingham, Strathclyde and Plymouth respectively. Currently, Reader in Electrical Power and Energy in the School of Engineering at the University of West of England. Areas of expertise are power systems analysis, lightning and transient analysis, power electronic applications to power systems, renewable energy integration and related issues, DC and AC microgrids, electric arc modeling and circuit breakers, fault locations, power quality, and smart grids. He can be contacted at email: nouri_h@ymail.com.